Earth Planets Space, **52**, 615–627, 2000

Spectral power of low-latitude Pi 2 pulsations at the 210° magnetic meridian stations and plasmaspheric cavity resonances

Ching-Chang Cheng[1], Jih-Kwin Chao[2], and Kiyohumi Yumoto[3]

[1]*Department of Physics, National Huwei Institute of Technology, Hu-Wei, Taiwan 63201, R.O.C.*
[2]*Institute of Space Science, National Central University, Chung-Li, Taiwan 32001, R.O.C.*
[3]*Department of Earth and Planetary Sciences, Kyushu University, 6-10-1 Hakozaki, Fukuoka 812-8581, Japan*

(Received March 15, 2000; Revised August 17, 2000; Accepted August 17, 2000)

Pi 2 pulsations at low latitudes are examined with magnetic fields data at the 210° magnetic meridian (MM) stations in 1991. Due to high degree of coherence over most latitudes, 68 low-latitude Pi 2 events at the 210° MM stations are identified with reference to same waveforms on the magnetogram at Lunping (189.5° MM, $L = 1.06$). With spectral power analysis, the ratio of the first four harmonic frequencies of low-latitude Pi 2 pulsations is about $1 : (1.7 \pm 0.1) : (2.3 \pm 0.1) : (2.9 \pm 0.1)$. By using a box model for the inner magnetosphere, the cold linearized MHD wave equations are studied with realistic Alfven speed profile for nonuniform ambient magnetic fields. With appropriate parameters to depict the magnetospheric environments during the aforementioned period, numerical results are acquired with the fourth order Runge-Kutta method. It is found that the ratio of the first four harmonic frequencies of plasmaspheric cavity resonances is about $1 : 1.7 : 2.4 : 3.1$ that is consistent with data analysis. This suggests that low-latitude Pi 2 pulsations at the 210° MM stations may be plasmaspheric cavity resonances driven by fast compressional waves owing to the impulsive source at the magnetotail.

1. Introduction

Pi 2 pulsations are impulsive, damped oscillations of geomagnetic field in the period range 40–150 seconds. This type of pulsations is predominantly a nighttime phenomenon (Yeoman *et al.*, 1994) and known to be associated with substorm onset (Saito *et al.*, 1976). Hence, Pi 2 pulsations are considered to result from hydromagnetic disturbances driven by a sudden change in magnetospheric convection or reconfiguration in the magnetotail during the substorm expansive phase (see review by Yumoto, 1986, 1988). However, it is not fully certain how Pi 2 pulsations propagate in the inner magnetosphere and how their frequencies are selected.

To explain latitude-dependent magnetic pulsations at the higher latitudes, field line resonances (FLRs) is widely believed to be a crucial mechanism in the wave coupling as distant source waves tunnel to excite the field line oscillations in the inner magnetosphere (Chen and Hasegawa, 1974a; Southwood, 1974). But Lanzerotti and Medford (1984) found that Pi 2 pulsations at low latitudes can't be explained with the FLRs theory and they suggested the possible source mechanism could be the substorm electrojet current wedge. Due to the orientation of the major axis of Pi 2 polarization directed to the center of the current wedge, the substorm current wedge is a possible source for mid-latitude Pi 2 pulsations (Lester *et al.*, 1989 and references there in). By comparing the spacecraft AMPTE/CCE and ground observations, however, statistical analysis of Pi 2 pulsations in the inner magnetosphere by Takahashi *et al.* (1995) show no evidence to support a view that ground Pi 2 pulsations at mid-latitudes ($2 < L < 5$) are resonant oscillations in response to the source waves on the auroral zone field line. Hence, the generation and propagation mechanisms of Pi 2 pulsations at lower latitudes seem different from those at higher latitudes.

Due to the rapid change of the Alfven speed on a boundary, there may exist surface waves of which the frequency is determined by the Alfven velocities on the both sides of the boundary (Chen and Hasegawa, 1974b). Thus, the source mechanism of mid-latitude Pi 2 pulsations might be associated with the surface waves at the plasmapause (Sutcliffe, 1975; Southwood and Stuart, 1980). On the other hand, early observations (e.g., Samson and Rostoker, 1972) reported that Pi 2 pulsations had the characteristics of discrete spectrum and suggested that there might exist global cavity modes. Recent observations pointed out that global cavity modes might be responsible for Pi 2 pulsations at very low latitudes and in the inner magnetosphere (Yumoto *et al.*, 1989; Yumoto, 1990; Lin *et al.*, 1991; Takahashi *et al.*, 1995).

For sake of the inhomogeneous distribution of the plasma and field configurations in the magnetosphere, fast compressional waves may couple to shear Alfven waves and cavity resonances would excite the resonant field line at low latitudes as the wave frequency is matched. Hence, many theoretical studies and numerical works have been focused on the spatial structure of the coupling of global cavity modes to FLRs (e.g., Kivelson and Southwood, 1986; Allan *et al.*, 1986; Zhu and Kivelson, 1989; Yumoto *et al.*, 1990; Fujita and Patel, 1992; Lee, 1996; and references there in). In order to explain the power distribution profile of Pi 2 pulsations in IGS chain (cf. Stuart, 1982), Cheng *et al.* (1998)

modified the box model proposed by Lin *et al.* (1991) and studied the irreversible hydromagnetic wave coupling in the magnetosphere. Due to consistence of numerical results with observations, Cheng *et al.* suggested that the coupling of a fast magnetospheric cavity mode to field line resonances is a possible scenario for low-latitude Pi 2 pulsations.

However, Stuart (1974) proposed that the secondary amplitude maximum of Pi 2 occurring between $L = 2.5$ and $L = 4$ is due to plasmaspheric cavity resonances. Moreover, using the magnetometer array from $L = 2.38$ to $L = 6.23$, Yeoman and Orr (1989) suggested that plasmaspheric cavity resonances is the most likely mechanism for the secondary amplitude maximum of mid-latitude Pi 2. Since the plasmapause is neither a good reflector nor a good transmitter, it is not well accepted that cavity resonances are driven by impulsive sources out of the plasmasphere. With analytical approach, Lee (1998) recently solved a radially propagating magnetohydrodynamic (MHD) wave equation based on the model of reasonable Alfven speed profile. The exact solution shows that plasmaspheric cavity modes strongly persist for arbitrary incoming impulses from the source in the magnetotail, which corresponding to Pi 2 pulsations. With availability of magnetic fields at the Akebono satellite and ground stations, Osaki *et al.* (1998) confirmed that Pi 2 puslations propagate to the ground from the magnetotail. By assuming that observed Pi 2 puslations represent the cavity mode, they found that the escaping Poynting flux could damp a cavity mode oscillations in ~10–20 s. In addition, Osaki *et al.* (1998) found that the transverse Pi 2 pulsations at the Akebono satellite last for 400 s. As a result, they argued that plasmaspheric cavity modes are not appropriate for Pi 2 pulsations in the plasmasphere. Thus, more observations and theoretical studies are needed to further clarify the generation and propagation mechanisms of Pi 2 pulsations at low latitudes.

In order to check the existing Pi 2 models, Yumoto *et al.* (1994) analyzed the magnetic field data from stations along the 210° magnetic meridian (MM). They found some properties of Pi 2 pulsations at low latitudes as follows. Pi 2 pulsations have similar waveforms at low latitudes. The H component of Pi 2 pulsations shows in phase at northern and southern stations. These suggest that FLRs cannot be used to explain low-latitude Pi 2. Hence, Yumoto *et al.* (1994) proposed that Pi 2 pulsations at the 210° MM stations might be cavity modes driven by fast compressional waves owing to the substorm onset. In this study, we attempt to use the box model by Cheng *et al.* (1998) to explain low-latitude Pi 2 pulsations at the 210° MM stations.

This paper is organized as follows. In Section 2, with reference to same waveforms at the Lunping station (LNP, 189.5° MM, $L = 1.06$), we examined magnetic field data at the 210° MM stations to confirm the observation of cavity-mode Pi 2. By using spectral analysis, the ratio of the first four harmonic frequencies of low-latitude Pi 2 at the 210° MM stations is presented. In Section 3, by using a box model for the inner magnetosphere, the cold linearized MHD waves equation is studied with realistic Alfven speed profile for nonuniform ambient magnetic fields. With appropriate parameters to depict the magnetospheric environments during the aforementioned period, numerical results are acquired with the fourth order Runge-Kutta method and compared to data analysis in Section 4. Finally, Section 5 discusses the possible source candidate for low-latitude Pi 2 pulsations and summarizes this study.

2. Data Presentation

In July of 1990, the Solar-Terrestrial Environment Laboratory at Nagoya University in Japan was led by Dr. Yumoto to install fluxgate magnetometers array at Moshiri (MSR) and Kagoshima (KAG) in Japan, and Adelaide (ADE), Birdsville (BRV), and Weipa (WEP) in Australia. Fluxgate magnetometer data from the Chichijima station (CBI) were obtained by courtesy of the Kakioka magnetic observatory. The fluxgate magnetometer observation at Guam (GAM) in USA was started in June of 1991. These stations are along the 210° MM (see Yumoto, 1996) and their locations are shown in Table 1. Due to all-year-round observation of magnetic pulsations at the 210° MM stations in 1991, it provides us an opportunity of analyzing statistically low-latitude Pi 2 pulsations.

In order to confirm the observation of cavity-mode Pi 2, we first inspect the dH/dt magnetogram at the LNP station. With reference to same waveforms at the LNP station, we identified Pi 2 events from magnetic field data at the 210° MM stations. It is shown in Fig. 1(a) that there is one Pi 2 event at the LNP station occurring at 12:37 UT (plus 8 hours corresponding to the local time 20:37 LT) on August 30, 1991. Same as Fig. 1(a), except for the occurrence time, it is shown in Fig. 1(b) that the other Pi 2 event occurred at 16:37 UT (24:37 LT). As reproduced from the dH/dt magnetogram at the LNP station, the relative amplitudes in Figs. 1(a) and (b) are not in the same scale as those at the 210° MM stations. On the other hand, it is shown in Fig. 2 that the unfiltered dH/dt components at the 210° MM stations are plotted from the north hemisphere to the south hemisphere.

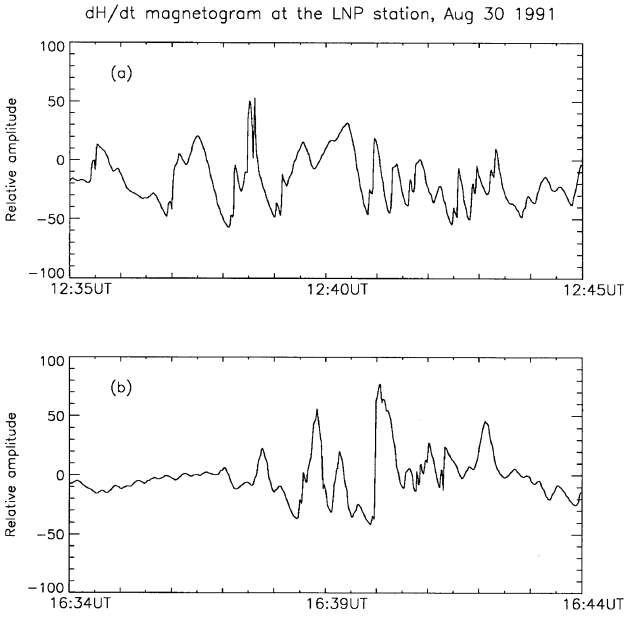

Fig. 1. An example of dH/dt magnetogram at the LNP station on August 30, 1991. (a) There is one Pi 2 event occurring at 12:37 UT. (b) Same as Fig. 1(a), except for the occurrence time at 16:37 UT.

Table 1. The locations of 210° MM stations and the Lunping station.

Station Name	Abbr.	Geographic Lat.	Geographic Long.	Geomagnetic Lat.	Geomagnetic Long.	L
Moshiri	MSR	44.37	142.27	37.76	212.96	1.6
Kagoshima	KAG	31.48	130.72	25.23	201.99	1.22
Chichijima	CBI	27.15	142.30	20.65	212.74	1.14
Lunping	LNP	25.00	121.17	13.80	189.50	1.06
Guam	GAM	13.58	144.87	9.02	215.18	1.03
Weipa	WEP	−12.68	141.88	−23.06	214.07	1.18
Birdsville	BRV	−25.83	139.33	−37.08	212.86	1.57
Adelaide	ADL	−34.67	138.65	−46.72	213.34	2.13

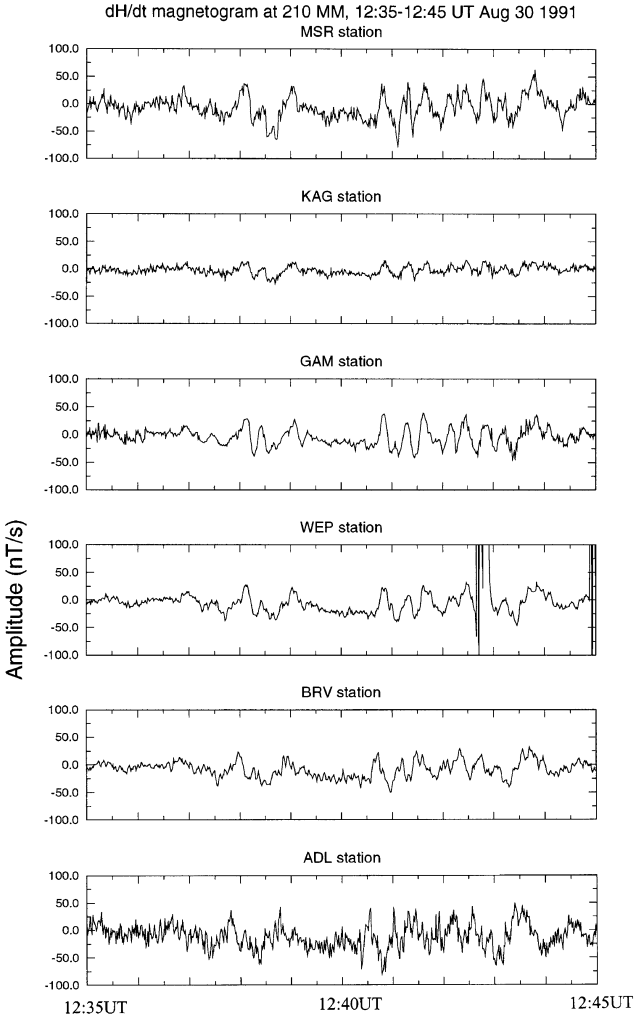

Fig. 2. An example of dH/dt magnetogram at the 210° MM stations between 12:35 UT and 12:45 UT on August 30, 1991. Same as Fig. 1(a), there are Pi 2 events occurring at 12:37 UT.

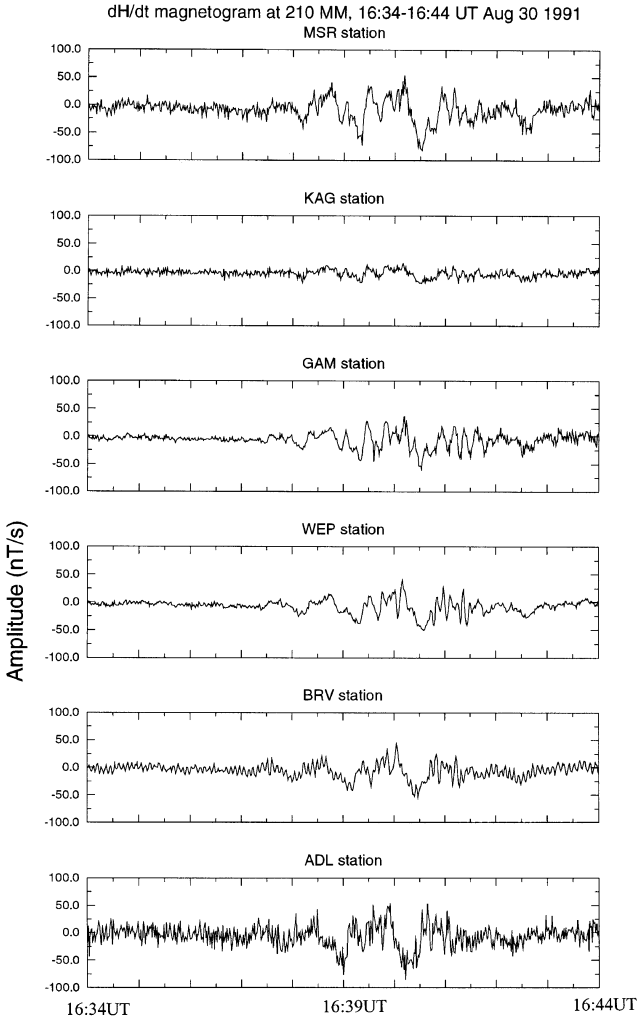

Fig. 3. An example of dH/dt magnetogram at the 210° MM stations between 16:34 UT and 16:44 UT on August 30, 1991. Same as Fig. 1(a), there are Pi 2 events occurring at 16:37 UT.

It is found from Fig. 2 that there are apparently same waveforms of Pi 2 events at the 210° MM stations as those at the LNP station with same occurrence times. It is also shown in Fig. 2 that for being less contaminated by noise, the waveform at the GAM station look more like those at the LNP station than other stations. Note that the local time at the 210° MM stations is the universal time plus 9 hours. Same as Fig. 2, except for the occurrence time, it is shown in Fig. 3

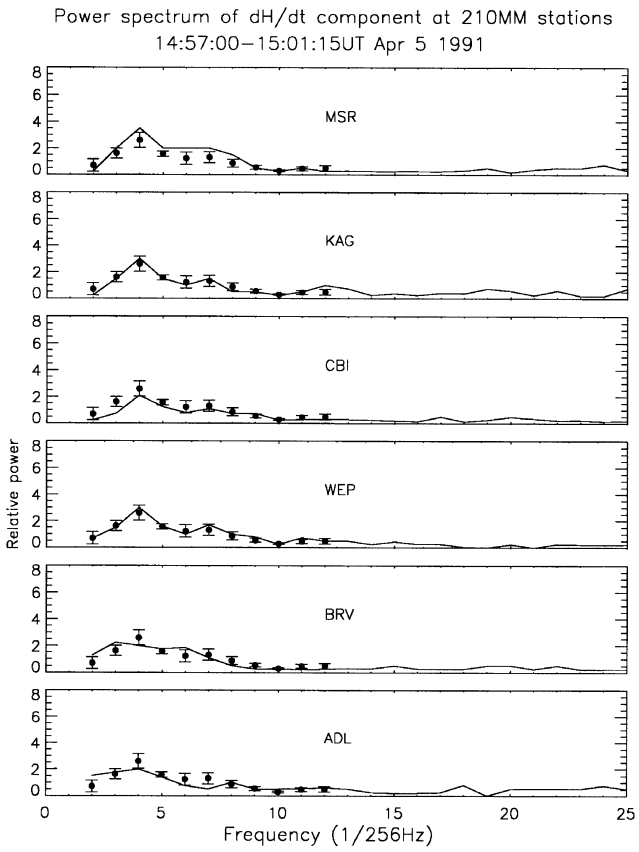

Fig. 4. An example of the power spectrum of dH/dt magnetogram at the 210° MM stations for one Pi 2 event occurring at 14:57 UT on April 5, 1991.

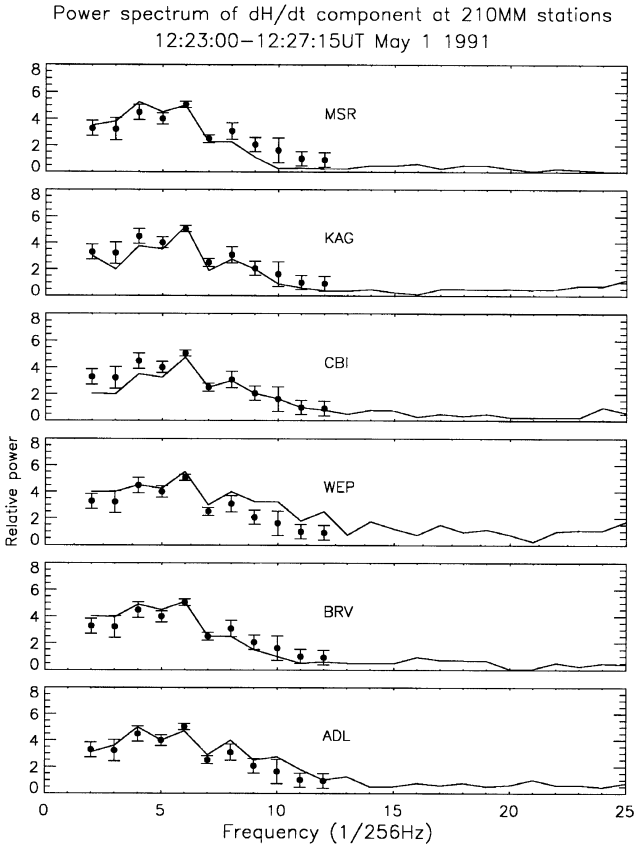

Fig. 5. Same as Fig. 4, except for one Pi 2 event occurring at 12:23 UT on May 1, 1991.

that from the north hemisphere to the south hemisphere, same waveforms of Pi 2 event at the 210° MM stations are similar to those at the LNP station occurring at the same universal time. It is also shown in Fig. 3 that the unfiltered dH/dt components at both GAM and WEP stations are less contaminated by noise. From Figs. 2 and 3, Pi 2 events at the LNP station are confirmed as cavity modes. Thus, Pi 2 pulsations at low latitudes can be selected from the unfiltered dH/dt component at the 210° MM stations with reference to same waveforms on the dH/dt magnetogram at the LNP station.

As mentioned in the introduction section, Pi 2 is predominantly a nighttime phenomenon. In this study, the time zone to select Pi 2 events is from 3 hours before midnight (referred as the pre-midnight zone henceforth) to 3 hours after midnight (referred as the post-midnight zone henceforth). This time zone corresponds to the night-side magnetospheric cavity in space that is same as one adopted to estimate the duration time of cavity-mode Pi 2 by Osaki *et al.* (1998). Following the selection criteria, 68 low-latitude Pi 2 events were selected from the unfiltered dH/dt component at the 210° MM stations in 1991. With no availability of digital dH/dt component at the LNP station, we only analyzed the spectral power of low-latitude Pi 2 pulsations at the 210° MM stations. For every Pi 2 event, 256 digitized data points are extracted from the unfiltered dH/dt component at the 210° MM stations and the sampled time is one second. Following Lin *et al.* (1991), we resort to use Fast Fourier Transform to analyze the power spectrum of Pi 2 event. As a result, Fig. 4 is an example of the power spectrum of low-latitude Pi 2 event at the 210° MM stations occurring at 14:57 UT, April 5, 1991. It is also shown in Fig. 4 that there are same power peaks at the frequency 4/256 Hz (corresponding to 64 s) at the 210° MM stations. Moreover, Figure 5 is another example of the power spectrum of low-latitude Pi 2 event at the 210° MM stations occurring at 12:23 UT, May 1, 1991. It is also shown in Fig. 5 that there are same dominant powers at the frequency 6/256 Hz (corresponding to 42 s) at the 210° MM stations. In addition, there are apparently four power peaks at both ADL and WEP stations in Fig. 5. This means that four power peaks at both ADL and WEP stations may result from the first four harmonic cavity modes. But there are three power peaks at other stations of which most are located in the north hemisphere except for the BRV station. The reason why the number of power peaks in the south hemisphere is different from the north hemisphere is remained unknown. Same as Lin *et al.* (1991), we refer to the first power peak as the first harmonic and the second power peak as the second harmonic etc. As a result, the frequency ratio of the second harmonic and the first harmonic versus the event number of low-latitude Pi 2 at the 210° MM stations is shown in Fig. 6. It is also shown in Fig. 6 that the shaded strip denotes the pre-midnight zone, the blank strip represents the post-midnight zone, and the solid strip includes the pre-midnight and post-midnight zones, respectively. It is obvious in Fig. 6 that the

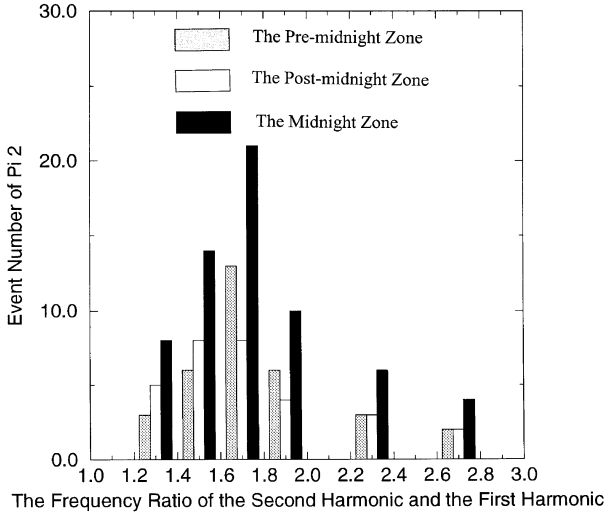

Fig. 6. A diagram of the frequency ratio of the second harmonic and the first harmonic versus the event number of Pi 2 at 210° MM stations in 1991. The shaded strip denotes the pre-midnight zone, the blank strip represents the post-midnight zone, and the solid strip includes the pre-midnight and post-midnight zones, respectively.

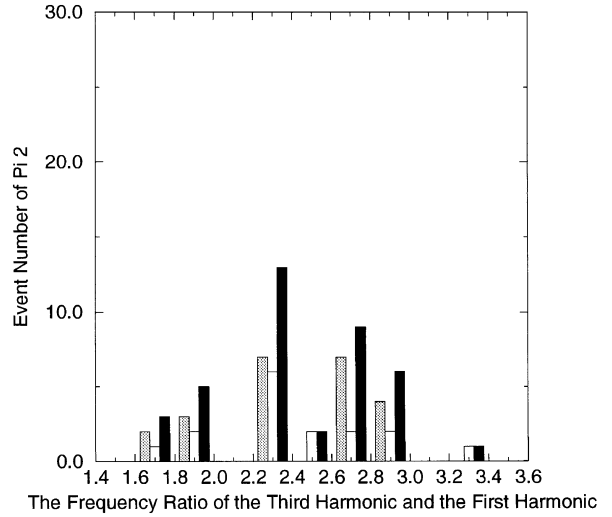

Fig. 7. Same as Fig. 6, except for the frequency ratio of the third harmonic and the first harmonic.

frequency ratio of the second harmonic and the first harmonic is about 1.6∼1.8 for the high event number. Same as Fig. 6, it is shown in Fig. 7 that the frequency ratio of the third harmonic and the first harmonic is about 2.2∼2.4 for the high event number. Same as Fig. 6, it is shown in Fig. 8 that the frequency ratio of the fourth harmonic and the first harmonic is about 2.8∼3.0 for the high event number. From Figs. 6 to 8, the frequency ratio of the first four harmonics is about $1 : (1.7 \pm 0.1) : (2.3 \pm 0.1) : (2.9 \pm 0.1)$. In the following section, the box model proposed by Cheng *et al.* (1998) is used to explain the observational result mentioned above.

3. The Box Model for the Inner Magnetosphere

In order to explain the observation of Pi 2 pulsations at $L = 1.06$, Lin *et al.* (1991) used the cold linearized MHD equations to estimate magnetospheric and plasmaspheric cavity

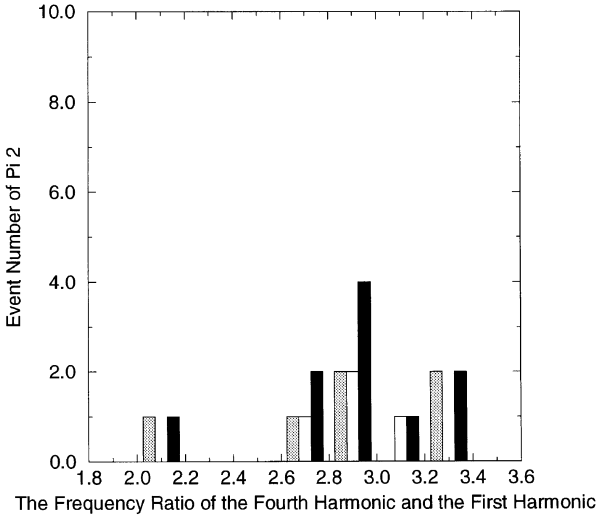

Fig. 8. Same as Fig. 6, except for the frequency ratio of the fourth harmonic and the first harmonic.

resonances, respectively. Since $\nabla \times \mathbf{B}_0 = 0$ in the dipole coordinate, the governing equation in their model is similar to the box model by Southwood (1974). However, Lin *et al.* treated the ambient magnetic field as a transformation of the dipole field for the equatorial plane and kept it straight like the box model. For the initial equilibrium, Cheng *et al.* (1998) modified the box model by assuming that there exists the plasma force $\mathbf{F}$ in the momentum equation to balance the magnetic force $\frac{1}{\mu_o}\mathbf{B}_0 \times (\nabla \times \mathbf{B}_0)$ where $\mathbf{B}_0$ is the ambient magnetic field and μ_o denotes the permeability in the free space. As a result, the cold linearized MHD equation of the perturbed electric field $\mathbf{E}_1$ can be obtained as follows:

$$\frac{d^2\mathbf{E}_1}{dt^2} = \frac{1}{\mu_o \rho_o}\big\{(\nabla \times \nabla \times \mathbf{E}_1) \times \mathbf{B}_0 \times \mathbf{B}_0 + (\nabla \times \mathbf{B}_0) \times (\nabla \times \mathbf{E}_1) \times \mathbf{B}_0\big\} \quad (1)$$

where ρ_o is the ambient plasma density.

In this study, the Cartesian coordinates are used to describe the box model. Let the origin point locate at the center of the Earth and the $+x$ axis directed antisunward. The direction of the $+z$ axis is along the Earth's magnetic fields. Finally, the $+y$ axis is directed toward the dawn. The radial distance x is in unit of the Earth's radius a. So that $x = a$ corresponds to the ionosphere at the low latitude and $x = ta$ corresponds to the site of impulsive sources in the magnetotail at the substorm expansive onset (see figure 1 of Cheng *et al.*, 1998). Moreover, $x = ta$ may correspond to the plasmapause location where incident fast compressional waves driven by impulsive sources in the magnetotail may be trapped inside. In order that fast compressional waves could reflect perfectly to excite a cavity resonance, the ionosphere is assumed as a perfect conductor in this study.

Since frozen-in effect in space plasma implies that the perturbed electric field $\mathbf{E}_1$ doesn't have z component, $\mathbf{E}_1$ can be assumed as

$$\mathbf{E}_1 = \big(E_{1x}(x), E_{1y}(x), 0\big) \exp\left[i(my + kz - \omega t)\right] \quad (2)$$

where E_{1y} is the electric field of the compressional wave and

E_{1x} corresponds to the toroidal component. In addition, m is the azimuthal wave number, k is the wave number along the z axis and ω is the wave frequency respectively.

Referring to Cheng *et al.* (1998), the ambient plasma density ρ_o is assumed as follows:

$$\rho_o(x) = \rho_p \cdot p^4 \cdot \left(\frac{a}{x}\right)^4 \qquad a \le x \le pa, \quad (3a)$$

$$\rho_o(x) = \rho_p \cdot p^6 \cdot \left(\frac{a}{x}\right)^6 \cdot \left[1 + \left(\frac{x}{a} - p\right)\frac{\sqrt{R}-1}{q-p}\right]^{-2} \qquad pa < x < qa, \quad (3b)$$

$$\rho_o(x) = \frac{1}{R} \cdot \rho_p \cdot p^4 \cdot \left(\frac{a}{x}\right)^4 \qquad qa \le x \le ta \quad (3c)$$

where ρ_p is the plasma density at the plasmapause, p is the L value at the plasmapause and R denotes the ratio of the plasma density drop. Same as Cheng *et al.* (1998), the ambient magnetic field is assumed as straight and varied radially as follows:

$$\mathbf{B}_0(x) = B_p \cdot p^3 \cdot \left(\frac{a}{x}\right)^3 \hat{z} \quad (4)$$

where B_p is the magnetic field at the plasmapause.

With (3) and (4), the Alfven speed $v_a = B_o/\sqrt{\mu_o \rho_o}$ can be described as follows:

$$v_a(x) = v_{ao} \cdot p \cdot \frac{a}{x} \qquad a \le x \le pa, \quad (5a)$$

$$v_a(x) = v_{ao} \cdot \left\{1 + \left(\frac{x}{a} - p\right)\frac{\sqrt{R}-1}{q-p}\right\} \qquad pa < x < qa, \quad (5b)$$

$$v_a(x) = \sqrt{R} \cdot v_{ao} \cdot p \cdot \frac{a}{x} \qquad qa \le x \le ta \quad (5c)$$

where v_{ao} is the Alfven speed at the plasmapause. Values of p, q, t and R are determined by the geomagnetic activity. Substituting (2), (3), (4) and (5) into (1), the governing equation can be obtained as follows:

$$\frac{d^2 E_{1y}}{dx^2} + \left\{\frac{2m^2\omega^2\left(\frac{dv_a}{dx}\right)}{\left(\frac{\omega^2}{v_a^2}\right)\left(\frac{\omega^2}{v_a^2} - k^2 - m^2\right)v_a^3} + \frac{1}{B_0}\frac{dB_0}{dx}\right\}\frac{dE_{1y}}{dx} + \left(\frac{\omega^2}{v_a^2} - k^2 - m^2\right)E_{1y} = 0. \quad (6)$$

There is no rigid boundary except for the Earth in the real magnetosphere to reflect fast compressional waves back to the magnetospheric cavity. Even for an apparent boundary like the dayside magnetopause, the perfect reflection is not easy for fast compressional waves propagating from the magnetosphere to the magnetosheath (Fujita and Patel, 1992). Recent studies (e.g., Allan *et al.*, 1986; Lee and Kim, 1999) also showed that the plasmapause is not often a rigid boundary. Therefore, some part of the wave energy in the magnetosphere/plasmasphere will be transmitted through the magnetospheric/plasmaspheric boundary. This means that the Poynting flux flows across the magnetospheric/plasmaspheric boundary might represent the energy loss of a fast magnetospheric/plasmaspheric cavity resonance. If the Poynting flux is responsible for the energy dissipation of a fast magnetospheric/plasmaspheric cavity resonance, the wave number should be a complex. Since most of the 210° MM stations are located in the same longitude, the damping of a fast magnetospheric/plasmaspheric cavity resonance could be investigated by adopting a complex frequency rather than a complex wave number and assumed as irreversible in this study.

Referring to Zhu and Kivelson (1988), the normal modes of a system can be obtained with two standard approaches. One approach is that the normal modes are inferred from the Green's function. The other approach is that the time variable is Fourier transformed and the properties of the normal modes are obtained as the eigenfunction and eigenvalues of a differential equation. It is hard to derive the Green's function in the realistic magnetosphere. Hence, the MHD waves equation is studied with the latter approach. In the classical FLR theory, the frequency of hydromagnetic perturbation is assumed as a complex with a negative imaginary ω_i. Similarly, $\gamma = \omega_i/\omega_r$ denotes the damping of fast magnetospheric/plasmaspheric cavity resonances and ω_r for the real part of the complex wave frequency. In this study, the electric perturbation E_{1y} in (6) is solved as a complex function with discrete ω_r and ω_i which are determined by the boundary condition.

At the substorm expansive onset, the density of plasma injection seems highly populated like the ionosphere. Hence, $x = ta$ corresponds to the position of plasma injection fronts that could be regarded as a perfect conductor at the substorm expansive onset. For fast compressional waves propagating between the low latitude ionosphere and plasma injection fronts, $E_{1y} = 0$ at $x = a$ and $x = ta$ are assumed as the boundary condition (cf., Kivelson and Southwood, 1988). Although the modeling of the magnetospheric substorm is still a controversial issue (Fairfield, 1992), the classical near-earth neutral line model is a well popular one. At the substorm expansive onset, the X-line is formed at $x \sim 10a$ in the tail (e.g., McPherron *et al.*, 1973). The tail reconnection would result from the formation of a X-line and launch plasma injection. Hence, $x = ta = 10a$ corresponding to the site of impulsive sources at the substorm expansive onset can be assumed as the tail boundary in this study.

On the other hand, Zhu and Kivelson (1989) proposed that fast compressional waves could be trapped between the low latitude ionosphere and the plasmapause. Even with consideration of the Poynting flux across the magnetospheric cavity boundary, Fujita and Glassmeier (1995) found that cavity resonance oscillations could be established in the plasmasphere. If the inner plasmasphere is in between larger potentials or Alfven speed barriers, Lee and Kim (1999) suggested that lowest frequencies of compressional waves would be trapped as virtual resonances. In other words, for the sharp density drop at the plasmapause, plasmaspheric cavity resonances would be driven by the impulsive source at the outer boundary in the magnetotail. If the impulsive source at the magnetotail could last for longer than the time to sustain plasmaspheric cavity resonances. The least outflow of Poynting flux along the meridian plane may lead to approximation of $E_{1y} = 0$ at

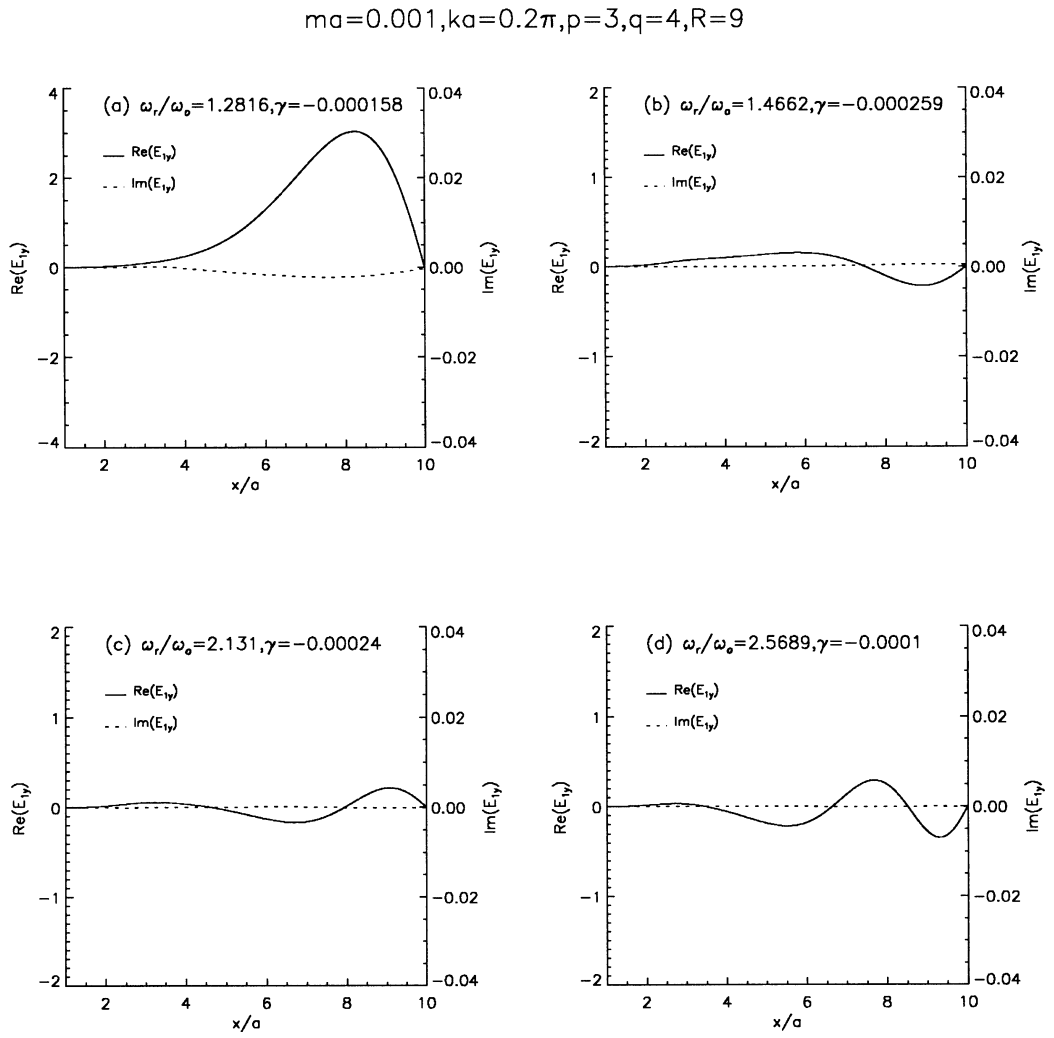

Fig. 9. (a) The profiles of the perturbed electric field E_{1y} of the fundamental magnetospheric cavity resonance in the radial direction obtained from the box magnetosphere for the inhomogeneous ambient magnetic field with $ma = 0.001$, $ka = 0.2\pi$, $p = 3$, $q = 4$, $R = 9$, $\omega_r/\omega_o = 1.2816$ and $\gamma = -0.000158$. The solid curve is for the real part of E_{1y} and the dashed curve for the imaginary part of E_{1y}. (b) Same as Fig. 9(a), except for the second magnetospheric cavity resonance and the eigenfrequency $\omega_r/\omega_o = 1.4662$ and $\gamma = -0.000259$. (c) Same as Fig. 9(a), except for the third magnetospheric cavity resonance and the eigenfrequency $\omega_r/\omega_o = 2.131$ and $\gamma = -0.00024$. (d) Same as Fig. 9(a), except for the fourth magnetospheric cavity resonance and the eigenfrequency $\omega_r/\omega_o = 2.5689$ and $\gamma = -0.0001$.

the plasmapause. But in the azimuthal direction, the outflow of Poynting flux becomes significant to damp plasmaspheric cavity resonances. As a result, it is feasible to explain low-latitude Pi 2 pulsations at the 210° MM stations by performing the calculation of plasmaspheric eigenmodes driven by impulsive sources near the plasmapause. By examining the plasma wave data acquired by the Akebono satellite, Osaki *et al.* (1998) inferred that the plasmapause location is about $L \sim 5$. Thus, the plasmapause location around $x = pa = 5a$ can be assumed as the plasmaspheric boundary in this study. Thus, $x = ta$ corresponds to the plasmapause location that can be also assumed as the boundary. Same as ω_r and ω_i, the damping factor $\gamma = \omega_i/\omega_r$ is discrete for satisfying the boundary condition that both the real part and the imaginary part of E_{1y} are simultaneously zero at $x = a$ and $x = ta$.

Near the midnight, the size of the impulsive source at the magnetotail is not actually a pinpoint (Takahashi *et al.*, 1995). Even the cross section area of BBF is about $3a \times 3a$ in the GSM y-z plane (Angelopoulos *et al.*, 1994). In addition, early ground measurements showed that azimuthal wave numbers of Pi 2 pulsations have a latitudinal dependence (see the review by Yumoto, 1986). It implies that azimuthal wave number m may not be exactly zero. By referring to previous simulation studies (e.g., Allan *et al.*, 1986), azimuthal wave number $ma = 0.001$ could be assumed to calculate cavity resonances in this study. Following Cheng *et al.* (1998), we solve (6) by adopting the fourth order Runge-Kutta method to estimate magnetospheric and plasmaspheric cavity resonances, respectively.

4. Is Low-Latitude Pi 2 at the 210° MM Stations Magnetospheric or Plasmaspheric Cavity Resonances?

In this study, both the Alfven speed v_a and the phase speed $v = \omega/k$ of hydromagnetic perturbations are normalized by v_{ao}. For convenience of calculation, the wavelength and the grid size are normalized by the Earth's radius a. The wave number k can be expressed as $ka = n\pi/l, n = 1, 2, 3, \ldots$

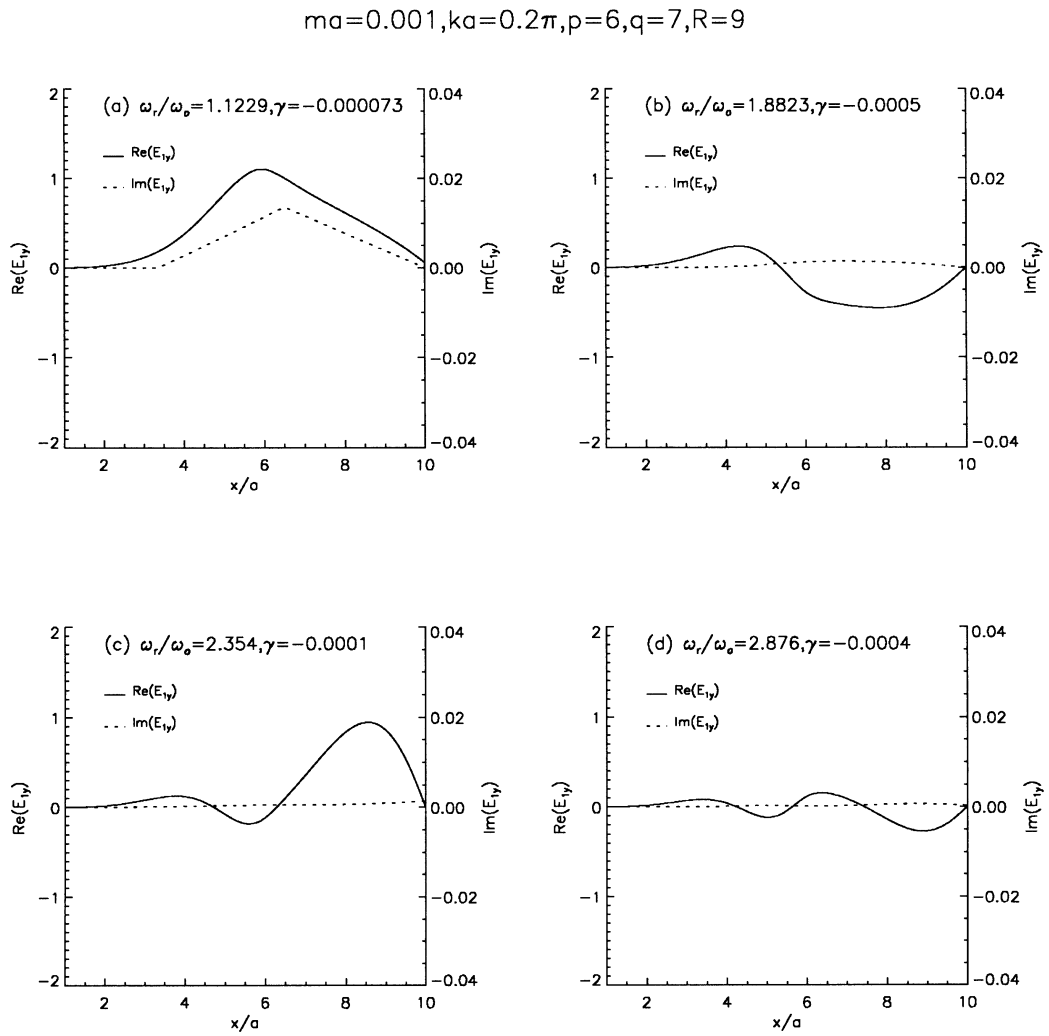

Fig. 10. (a) The profiles of the perturbed electric field E_{1y} of the fundamental magnetospheric cavity resonance in the radial direction obtained from the box magnetosphere for the inhomogeneous ambient magnetic field with $ma = 0.001$, $ka = 0.2\pi$, $p = 6$, $q = 7$, $R = 9$, $\omega_r/\omega_o = 1.1229$ and $\gamma = -0.000073$. The solid curve is for the real part of E_{1y} and the dashed curve for the imaginary part of E_{1y}. (b) Same as Fig. 10(a), except for the second magnetospheric cavity resonance and the eigenfrequency $\omega_r/\omega_o = 1.8823$ and $\gamma = -0.0005$. (c) Same as Fig. 10(a), except for the third magnetospheric cavity resonance and the eigenfrequency $\omega_r/\omega_o = 2.354$ and $\gamma = -0.0001$. (d) Same as Fig. 10(a), except for the fourth magnetospheric cavity resonance and the eigenfrequency $\omega_r/\omega_o = 2.876$ and $\gamma = -0.0004$.

where $l = 5$ is the normalized length of the magnetic field line same as figure 1 of Cheng *et al.* (1998). Henceforth, ma denotes the azimuthal wave number m. Cavity resonances are calculated for $n = 1$ with reference to in-phase of B_{1x} component of Pi 2 pulsations on AMPTE/CCE in both hemispheres (Takahashi *et al.*, 1995). Note that $\omega_o = v_{ao}/a$, the real part frequency of cavity resonances is normalized by ω_o. The electric perturbation E_{1y} of the first four magnetospheric cavity resonances is calculated for $ka = 0.2\pi$, $ma = 0.001$, $p = 3$, $q = 4$, $t = 10$ and $R = 9$. In Fig. 9, the solid curve is for the real part of E_{1y} and the dashed curve for the imaginary part of E_{1y}. Figure 9(a) shows the fundamental magnetospheric cavity resonance for $\omega_r/\omega_o = 1.2816$ and $\gamma = -0.000158$. Same as Fig. 9(a), Figure 9(b) shows the second magnetospheric cavity resonance for $\omega_r/\omega_o = 1.4662$ and $\gamma = -0.000259$. Same as Fig. 9(a), Figure 9(c) shows the third magnetospheric cavity resonance for $\omega_r/\omega_o = 2.131$ and $\gamma = -0.00024$. Same as Fig. 9(a), Figure 9(d) shows the fourth magnetospheric cavity resonance for $\omega_r/\omega_o = 2.5689$ and $\gamma = -0.0001$. From Figs. 9(a) to (d), the frequency ratio of the first four magnetospheric cavity resonances is about $1 : 1.4 : 1.6 : 2.3$. Same as Fig. 9, Figure 10 shows the electric perturbation E_{1y} of the first four magnetospheric cavity resonances for $ka = 0.2\pi$, $ma = 0.001$, $p = 6, q = 7, t = 10$ and $R = 9$. Figure 10(a) shows the fundamental magnetospheric cavity resonance for $\omega_r/\omega_o = 1.1229$ and $\gamma = -0.000073$. Same as Fig. 10(a), Figure 10(b) shows the second magnetospheric cavity resonance for $\omega_r/\omega_o = 1.8823$ and $\gamma = -0.0005$. Same as Fig. 10(a), Figure 10(c) shows the third magnetospheric cavity resonance for $\omega_r/\omega_o = 2.354$ and $\gamma = -0.0001$. Same as Fig. 10(a), Figure 10(d) shows the fourth magnetospheric cavity resonance for $\omega_r/\omega_o = 2.876$ and $\gamma = -0.0004$. From Figs. 10(a) to (d), the frequency ratio of the first four magnetospheric cavity resonances is about $1 : 1.7 : 2.1 : 2.6$. The magnetospheric cavity resonances for other possible values of the plasmapause location are also estimated but not shown in this paper. The frequency ratios of the first four

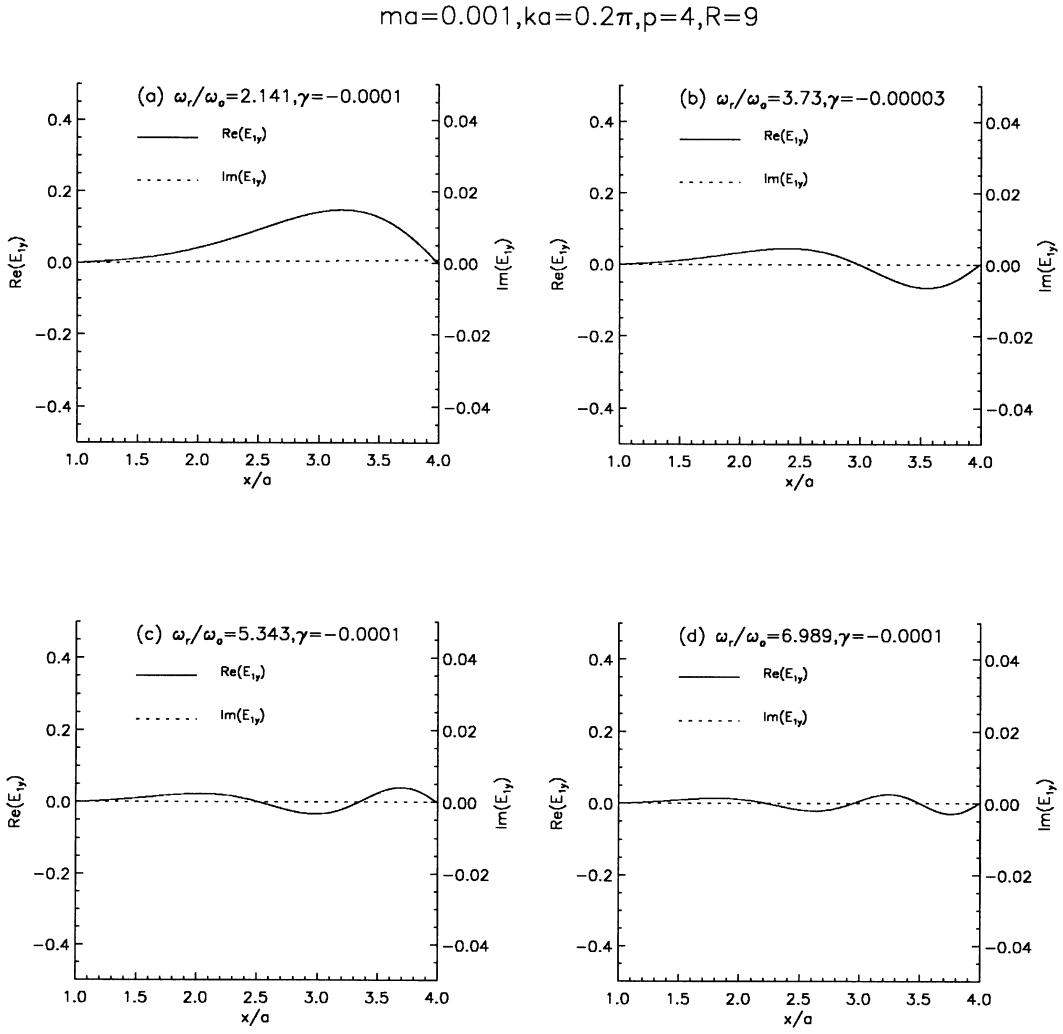

Fig. 11. (a) The profiles of the perturbed electric field E_{1y} of the fundamental plasmaspheric cavity resonance in the radial direction obtained from the box plasmasphere for the inhomogeneous ambient magnetic field with $ma = 0.001$, $ka = 0.2\pi$, $p = 4$, $R = 9$, $\omega_r/\omega_o = 2.141$ and $\gamma = -0.0001$. The solid curve is for the real part of E_{1y} and the dashed curve for the imaginary part of E_{1y}. (b) Same as Fig. 11(a), except for the second plasmaspheric cavity resonance and the eigenfrequency $\omega_r/\omega_o = 3.73$ and $\gamma = -0.00003$. (c) Same as Fig. 11(a), except for the third plasmaspheric cavity resonance and the eigenfrequency $\omega_r/\omega_o = 5.343$ and $\gamma = -0.0001$. (c) Same as Fig. 11(a), except for the fourth plasmaspheric cavity resonance and the eigenfrequency $\omega_r/\omega_o = 6.989$ and $\gamma = -0.0001$.

magnetospheric cavity resonance are about 1 : 1.1 : 1.6 : 2.0 for $p = 4$, $q = 5$ and 1 : 1.5 : 1.8 : 2.4 for $p = 5$, $q = 6$, respectively. These numerical results are inconsistent with data analysis at the 210° MM stations. It means that magnetospheric cavity resonances may not be responsible for low-latitude Pi 2 pulsations at the 210° MM stations.

If fast compressional waves are trapped between the low latitude ionosphere and the plasmapause, cavity resonances could be excited in the plasmasphere. Hence, we attempt to calculate the frequency ratio of plasmaspheric cavity resonances by using the box model for the plasmasphere instead. Therefore, $E_{1y} = 0$ at $x = a$ and $x = ta = pa$ are assumed as the boundary condition in the plasmaspheric cavity. Same as Fig. 9, except for the plasmaspheric cavity, Figure 11 shows the electric perturbation E_{1y} of the first four plasmaspheric cavity resonances for $ka = 0.2\pi$, $ma = 0.001$, $p = 4$ and $R = 9$. Figure 11(a) shows the fundamental plasmaspheric cavity resonance for $\omega_r/\omega_o = 2.141$ and $\gamma = -0.0001$. Same as Fig. 11(a), Figure 11(b) shows the second plasmaspheric cavity resonance for $\omega_r/\omega_o = 3.73$ and $\gamma = -0.00003$. Same as Fig. 11(a), Figure 11(c) shows the third plasmaspheric cavity resonance for $\omega_r/\omega_o = 5.343$ and $\gamma = -0.0001$. Same as Fig. 11(a), Figure 11(d) shows the fourth plasmaspheric cavity resonance for $\omega_r/\omega_o = 6.989$ and $\gamma = -0.0001$. From Figs. 11(a) to (d), the frequency ratio of the first four plasmaspheric cavity resonances is about 1 : 1.7 : 2.5 : 3.3. Same as Fig. 11, except for the plasmapause location, Figure 12 shows the electric perturbation E_{1y} of the first four plasmaspheric cavity resonances for $ka = 0.2\pi$, $ma = 0.001$, $p = 5$ and $R = 9$. Figure 12(a) shows the fundamental plasmaspheric cavity resonance for $\omega_r/\omega_o = 1.7895$ and $\gamma = -0.00021$. Same as Fig. 12(a), Figure 12(b) shows the second plasmaspheric cavity resonance for $\omega_r/\omega_o = 3.024$ and $\gamma = -0.0003$. Same as Fig. 12(a), Figure 12(c) shows the third plasmaspheric cavity resonance for $\omega_r/\omega_o = 4.281$ and $\gamma = -0.0001$. Same as Fig. 12(a), Figure 12(d) shows the fourth plasmaspheric cavity resonance for $\omega_r/\omega_o = 5.555$ and $\gamma = -0.00001$.

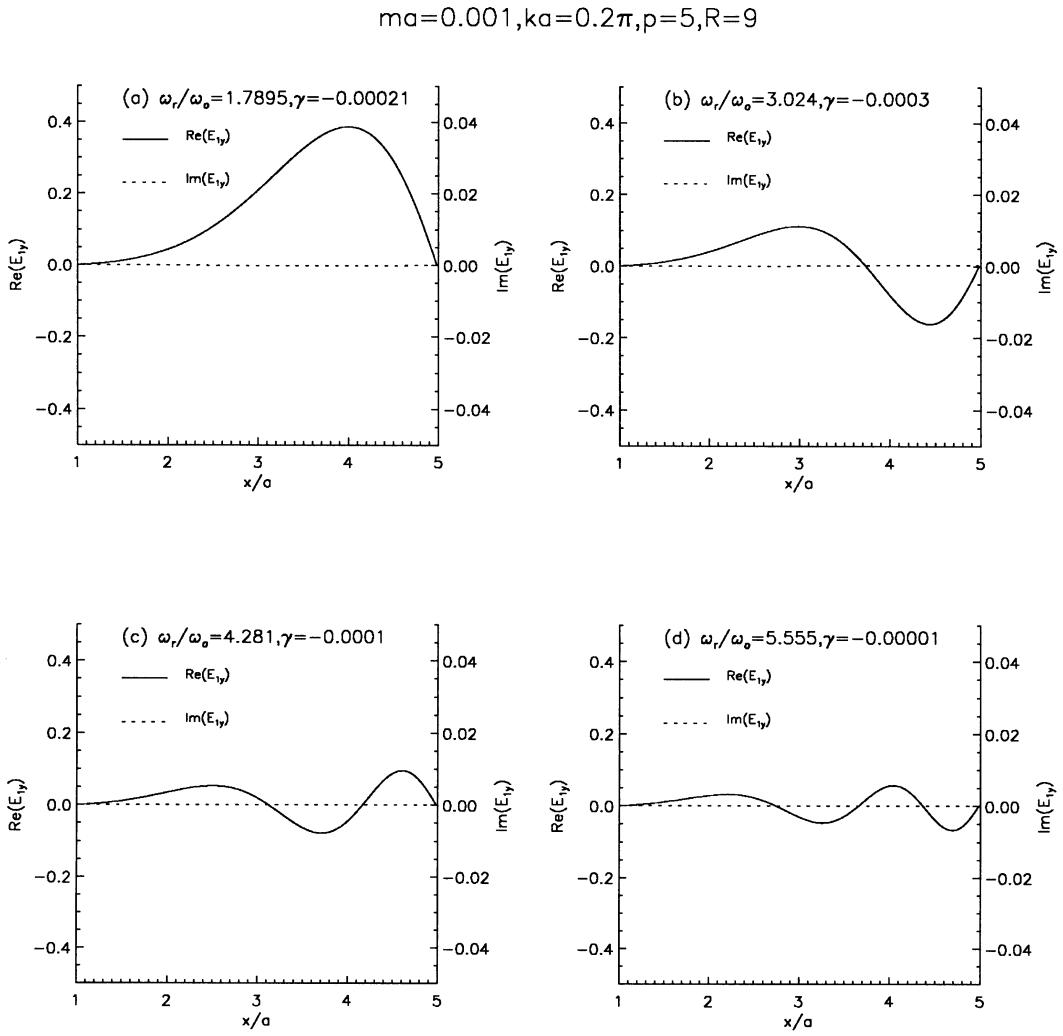

Fig. 12. (a) The profiles of the perturbed electric field E_{1y} of the fundamental plasmaspheric cavity resonance in the radial direction obtained from the box plasmasphere for the inhomogeneous ambient magnetic field with $ma = 0.001$, $ka = 0.2\pi$, $p = 5$, $R = 9$, $\omega_r/\omega_o = 1.785$ and $\gamma = -0.00021$. The solid curve is for the real part of E_{1y} and the dashed curve for the imaginary part of E_{1y}. (b) Same as Fig. 12(a), except for the second plasmaspheric cavity resonance and the eigenfrequency $\omega_r/\omega_o = 3.024$ and $\gamma = -0.0003$. (c) Same as Fig. 12(a), except for the third plasmaspheric cavity resonance and the eigenfrequency $\omega_r/\omega_o = 4.281$ and $\gamma = -0.0001$. (d) Same as Fig. 12(a), except for the fourth plasmaspheric cavity resonance and the eigenfrequency $\omega_r/\omega_o = 5.555$ and $\gamma = -0.00001$.

From Figs. 12(a) to (d), the frequency ratio of the first four plasmaspheric cavity resonances is about 1 : 1.7 : 2.4 : 3.1. The plasmaspheric cavity resonances for other possible values of the plasmapause location are also estimated but not shown in this paper. The frequency ratios of the first four plasmaspheric cavity resonances are about 1 : 1.6 : 2.3 : 3.0 for $p = 6$ and 1 : 1.6 : 2.2 : 2.8 for $p = 7$, respectively. These numerical results especially for $p = 5$ and $p = 6$ are consistent with data analysis at the 210° MM stations. It is apparent that plasmaspheric cavity resonances may be the source mechanism of low-latitude Pi 2 pulsations at the 210° MM stations.

In this study, plasmaspheric cavity resonances are two-dimensional oscillations of which eigenfrequencies depend upon the plasmapause location p and the wave number k. Note that the wave number k is determined by the field-aligned wavelength λ/a. To verify whether the plasmapause location play more dominant role on determining the frequency ratios of the first four plasmaspheric cavity resonances than the field-aligned wavelength, we recalculated their frequency ratios with different plasmapause locations and various field-aligned wavelengths for same $ma = 0.001$ and $R = 9$, respectively. It is shown in Fig. 13(a) that the frequency ratios of the first four plasmaspheric cavity resonances for the plasmapause location at $p = 4$ are versus to the field-aligned wavelength λ/a that varies from 5 to 10. The solid curve is for the ratio of ω_{r2}/ω_{r1}, the dotted curve for the ratio of ω_{r3}/ω_{r1} and the dashed curve for the ratio of ω_{r4}/ω_{r1}. Same as Fig. 13(a), except for the plasmapause location, Figure 13(b) shows the frequency ratios of the first four plasmaspheric cavity resonances for the plasmapause location at $p = 5$. Same as Fig. 13(a), except for the plasmapause location, Figure 13(c) shows the frequency ratios of the first four plasmaspheric cavity resonances for the plasmapause location at $p = 6$. Same as Fig. 13(a), except for the plasmapause location, Figure 13(d) shows the frequency ratios of the first four plasmaspheric cavity resonances for the plasmapause location at $p = 7$. From Figs. 13(a) to (d), it is

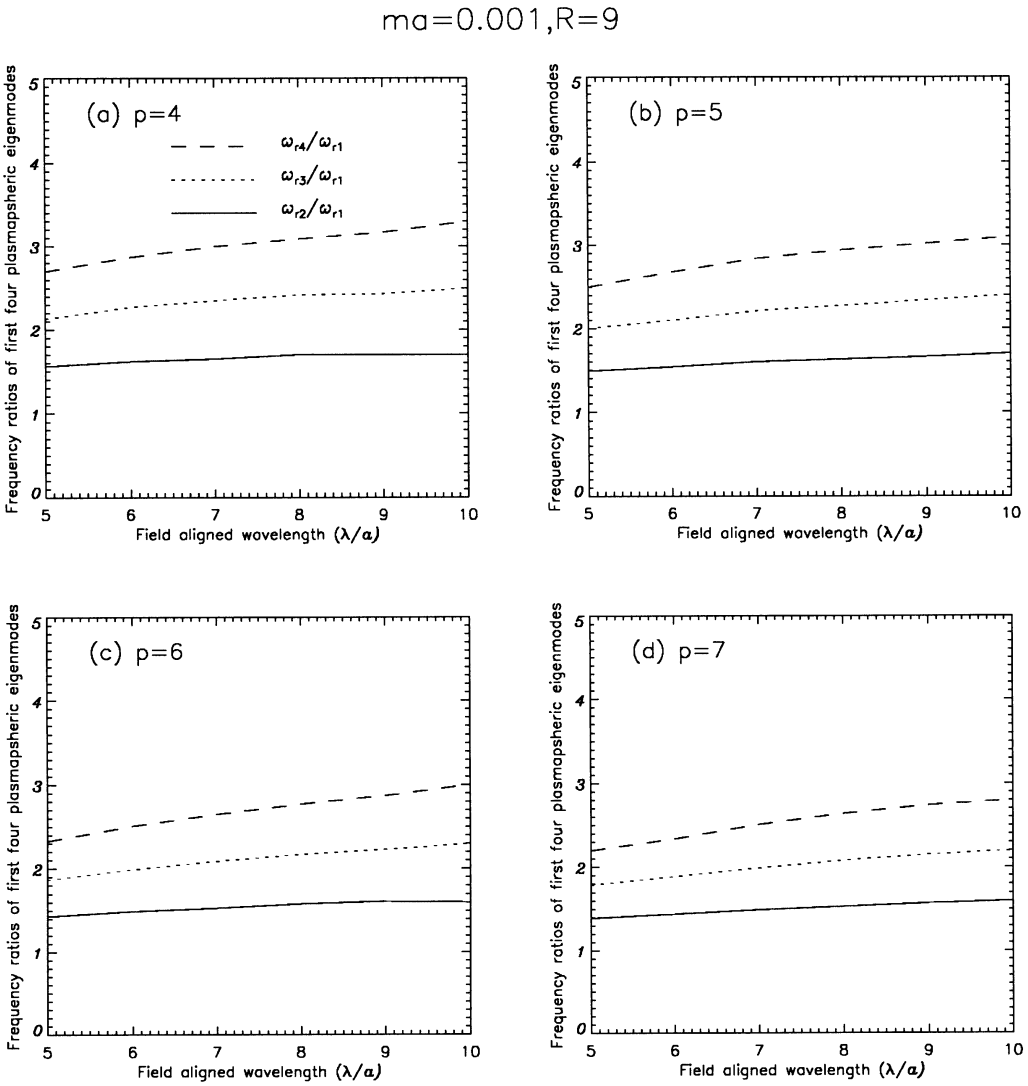

Fig. 13. (a) The profiles of the frequency ratios of the first four plasmaspheric cavity resonances obtained with various field-aligned wavelengths for $ma = 0.001$, $p = 4$ and $R = 9$. The solid curve is for the ratio of ω_{r2}/ω_{r1}, the dotted curve for the ratio of ω_{r3}/ω_{r1} and the dashed curve for the ratio of ω_{r4}/ω_{r1}. (b) Same as Fig. 13(a), except for the plasmaspause location at $p = 5$. (c) Same as Fig. 13(a), except for the plasmaspause location at $p = 6$. (d) Same as Fig. 13(a), except for the plasmaspause location at $p = 7$.

apparent that the field-aligned wavelength seems to play less dominant role on determining the frequency ratios of the first four plasmaspheric cavity resonances than the plasmapause location.

5. Discussion and Summary

Among previous studies (e.g., Lin *et al.*, 1991; Itonaga *et al.*, 1992), only observational results of three harmonics of Pi 2 events at low latitudes were examined and not fully explained with the plasmaspheric cavity resonances model. Especially Itonaga *et al.* (1992) studied the discrete spectral structure of low-latitude and equatorial Pi 2 pulsations with a maximum likelihood method. They found three components with the almost identical frequencies in the event simultaneously observed at the stations with a larger longitudinal separation. Except for equatorial stations, Itonaga *et al.* (1992) also found the fourth component of Pi 2 at the low-latitude station. But this component is a growing sinusoid and might be caused by reducing computational time. Moreover, the frequency ratios of first three harmonics of low-latitude Pi 2 by Itonaga *et al.* (1992) are different from our observational results. Hence, to our knowledge, there are few observational evidences of four harmonics of Pi 2 events at low-latitudes. The spectral power of low-latitude Pi 2 pulsations at 210° MM is a new finding and observational fact.

To justify whether Figure 12 could explain the power spectra of low-latitude Pi 2 pulsations at the 210° MM stations, we have to estimate the period of cavity resonances with specific parameters. Lin *et al.* (1991) derived a formula to estimate the period of cavity resonances

$$T = \frac{59 \times 10^{-6} p^3 (m_i/m_p)^{1/2} (n_o)^{1/2}}{\omega_c} \text{s} \qquad (7)$$

where m_i/m_p is the ratio of the average ion mass to the proton mass, n_o is the plasma number density at the plasmapause and $\omega_c = \omega_r/\omega_o$ is the normalized frequency of cavity resonances. The corresponding period of the fundamental plasmaspheric cavity resonance obtained by taking $\omega_c = 1.7895$,

$p = 5, m_i/m_p = 7.2$ and $n_o = 40 \times 10^6 \mathrm{m}^{-3}$ into (7) is about $T = 69.7$ s. Similarly, the corresponding period of the second plasmaspheric cavity resonance is $T = 41.2$ s by taking $\omega_c = 3.024$ with the same values of p, m_i/m_p and n_o into (7). It is obvious that the periods of the fundamental and second plasmaspheric cavity resonances in Fig. 12 are in the period range of Pi 2 pulsations and consistent with the dominant harmonic frequencies of low-latitude Pi 2 pulsations at the 210° MM stations (see Figs. 4 and 5). Except for the different plasmaspheric cavity resonances model, these periods are close to those of the first and second harmonics Pi 2 event observed by Lin *et al.* (1991), and the second and third components in the Itonaga *et al.* (1992) study. They are also similar to those of two power peaks in the virtual plasmaspheric resonances solved by Lee (1998) with an analytical box model. However, Fujita *et al.* (2000) recently studied the transient response of impulse source in the realistic magnetosphere model. Their results show that the electric field of the fundamental mode does not have a node at the plasmapause. Thus, they argued that there might exist plasmaspheric virtual resonances as Lee (1998) proposed. With limited events in this study, it is hard to discern which mechanism plays a dominant role on low-latitude Pi 2 pulsations. Nevertheless, it is an interesting topic for the future study to determine the source mechanism for low-latitude Pi 2 pulsations with investigation of the comparison between the plasmaspheric cavity resonances model and the plasmaspheric virtual resonances model. As a result, low-latitude Pi 2 pulsations at the 210° MM stations may be plasmaspheric cavity resonances driven by the impulsive sources associated with the substorm expansive onset in the magnetotail. This scenario is similar to one proposed by Yumoto *et al.* (1989).

Unlike the cylinder and dipole models, the box model is mathematically tractable to quantitatively compare with the observational result. Hence, it is a preliminary step to estimate the harmonic frequency of cavity resonances by simplifying the inner magnetospheric cavity as a rectangular box. However, the dominant harmonic frequencies of low-latitude Pi 2 pulsations at the 210° MM stations are consistent with those of cavity waves in the box model. Indeed, plasmaspheric cavity resonances are two-dimensional oscillations due to dipolar geometry on the meridian plane. But it is shown in Fig. 13 that the field-aligned wavelength seems to play less dominant role on determining the frequency ratios of plasmaspheric cavity resonances than the plasmapause location. It indicates that the dominant frequencies of low-latitude Pi 2 pulsations may be determined mainly in one-dimensional scale along the radial direction of the real dipolar inner magnetosphere.

Note that the periods of higher harmonics of Pi 2 events at the 210° MM stations are shorter than their typical period. This implies that the source mechanism for low-latitude Pi 2 pulsations at 210° MM stations may not be compressional eigenmodes only. Until now, it is still a controversial issue on the source mechanism for Pi 2 pulsations at middle and low latitudes. With the simultaneous occurrence of Pi 2 pulsations at ground stations separated in wide longitudes and latitudes, early studies (e.g., Yeomann and Orr, 1989; Sutcliffe and Yumoto, 1991; Itonaga *et al.*, 1992) proposed that they might be magnetospheric/plasmaspheric cavity resonances. But it seems difficult to maintain one-dimensional cavity resonance in the plasmasphere (i.e., $E_{1y} = 0$ at the plasmapause) since the plasma density is lower outside the plasmapause. With analysis of waveforms, Itonaga *et al.* (1997) pointed out that one-dimensional cavity-mode resonances are not the sole dominant constituent for low-latitude and equatorial Pi 2 pulsations. They argued that some constituents of Pi 2 pulsations might be quasi-steady-state oscillations forced by an oscillatory source outside the plasmasphere. With the energy budget consideration for plasmaspheric cavity modes, Osaki *et al.* (1998) suggested that the oscillation source for Pi 2 at Akebono is external to the plasmasphere. Recently, by using comparison with ground and space observations, Kepko and Kivelson (1999) reported that there is a direct link between middle- and low-latitude Pi 2 pulsations and Bursty Bulk Flows (BBFs) in the magnetotail. They also found that mid-latitude Pi 2 on the nightside is a precursor to indicate the occurrence of enhanced earthward flow bursts from the magnetotail. Due to geomagnetic dipolization in the inner nightside magnetosphere, the braking of enhanced earthward flow bursts from the magnetotail may lead to the formation of the substorm current wedge. As a result, mid-latitude Pi 2 may be the transient response of the ionosphere to the substorm current wedge. However, there is no direct evidence that nightside Pi 2 pulsations at low latitudes are correlated with the BBF except for the flank. According to their study, the BBF has not only large V_x component but also significant V_y component. The V_y component would divert the BBF to the flank before approaching the plasmapause. Thus, Kepko and Kivelson (1999) proposed that the BBF compressed the flux tube in the inner magnetosphere so that the compressional disturbance propagated down to the ground as low-latitude Pi 2 pulsations on the flank. But the median duration time of the earthward BBF is about ~550 s (Angelopoulos *et al.*, 1994) and it's typical speed is about 1000 km/s (cf., Kepko and Kivelson, 1999). From the reconnection site at the magnetotail, the BBF with larger V_x component and negligible V_y component may flow close to the plasmapause in about ~40 s. Since the typical Alfven speed at the plasmapause is about 2000 km/s (cf., Lee and Kim, 1999), the flight time to sustain the fundamental cavity resonance in the plasmaphere is about ~32 s. After the substorm expansive onset, the braking of BBF near the plasmapause may launch compressional waves to occupy the plasmaspheric cavity and excite cavity resonance during its duration time. According to Kepko and Kivelson (1999), the BBF has a period of ~50s which is close to those of the third components of Pi 2 event in the Itonaga *et al.* (1992) study and the second harmonics (see Fig. 5) in this study. Hence, it cannot rule out the possibility that the BBF may be a possible source candidate for low-latitude Pi 2 pulsations. The well-coordinated simultaneous measurements on the ground and in space are needed for further verification of the source mechanism of Pi 2 pulsations at low latitudes.

In this study, Pi 2 pulsations at low latitudes are examined with magnetic fields data at the 210° MM stations in 1991. Due to high degree of coherence over most latitudes, 68 low-latitude Pi 2 events at the 210° MM stations are identified with reference to same waveforms on the magnetogram at Lunping. With spectral power analysis, the ratio of the first

four harmonic frequencies of low-latitude Pi 2 pulsations is about $1 : (1.7 \pm 0.1) : (2.3 \pm 0.1) : (2.9 \pm 0.1)$. By using a box model for the inner magnetosphere, the cold linearized MHD wave equations is studied with realistic Alfven speed profile for nonuniform ambient magnetic fields. With appropriate parameters to depict the magnetospheric environments during the aforementioned period, numerical results are acquired with the fourth order Runge-Kutta method. It is found that the ratio of the first four harmonic frequencies of plasmaspheric cavity resonances is about $1 : 1.7 : 2.4 : 3.1$ that is consistent with data analysis. This suggests that low-latitude Pi 2 pulsations at the 210° MM stations may be plasmaspheric cavity resonances driven by fast compressional waves owing to the impulsive source at the magnetotail.

Acknowledgments. We are greatly indebted to both referees for their comments and suggestions. We thank Dr. Y. M. Huang and Mr. C. S. Chen for the magnetogram at the Lunping observatory. We also thank all members of the 210° MM Magnetic Observation Group for their ceaseless supports. The 210° MM database was made in the STEL, Nagoya University, Japan. This work was supported by the National Science Council of R.O.C. in Taiwan under grant NSC 89-2111-M-150-001.

References

Allan, W., S. P. White, and E. M. Poulter, Impulsive-excited hydromagnetic cavity and field-line resonances in the magnetosphere, *Planet. Space Sci.*, **34**, 371–385, 1986.

Angelopoulos, V., C. F. Kennel, F. V. Coroniti, R. Pellat, M. G. Kivelson, R. J. Walker, C. T. Russell, W. Baumjohann, W. C. Feldman, and T. J. Gosling, Statistical characteristics of bursty bulk flow events, *J. Geophys. Res.*, **99**, 21257–21280, 1994.

Chen, L. and A. Hasegawa, A theory of long-period magnetic pulsations, 1, Steady state excitation of field line resonances, *J. Geophys. Res.*, **79**, 1024–1032, 1974a.

Chen, L. and A. Hasegawa, A theory of long-period magnetic pulsations, 2, Impulse excitation of surface eigenmode, *J. Geophys. Res.*, **79**, 1033–1037, 1974b.

Cheng, C.-C., J.-K. Chao, and T.-S. Hsu, Evidence of the coupling of a fast magnetospheric cavity mode to field line resonances, *Earth Planets Space*, **50**, 683–697, 1998.

Fairfield, D. H., Advances in magnetospheric storm and substorm research: 1989–1991, *J. Geophys. Res.*, **97**, 10865–10874, 1992.

Fujita, S. and K. H. Glassmeier, Magnetospheric cavity resonance oscillations with energy flow across the magnetopause, *J. Geomag. Geoelectr.*, **47**, 1277–1292, 1995.

Fujita, S. and V. L. Patel, Eigenmode analysis of coupled magnetohydrodynamic oscillations in the magnetosphere, *J. Geophys. Res.*, **97**, 13777–13788, 1992.

Fujita, S., M. Itonaga, and H. Nakata, Relationship between the Pi2 pulsations and the localized impulsive current associated with the current disruption in the magnetosphere, *Earth Planets Space*, **52**, 267–281, 2000.

Itonaga, M., T.-I. Kitamura, O. Saka, H. Tachihara, M. Shinohara, and A. Yoshikawa, Discrete spectral structure of low-latitude and equatorial Pi 2 pulsation, *J. Geomag. Geoelectr.*, **44**, 253–259, 1992.

Itonaga, M., A. Yoshikawa, and K. Yomoto, One-dimensional transient response of the inner magnetosphere at the magnetic equator, 2, Analysis of waveforms, *J. Geomag. Geoelectr.*, **49**, 49–68, 1997.

Kepko, L. and M. G. Kivelson, Generation of Pi 2 pulstions by bursty bulk flows, *J. Geophys. Res.*, **104**, 25021–25034, 1999.

Kivelson, M. G. and D. J. Southwood, Coupling of Global magnetospheric MHD eigenmodes to field line resonances, *J. Geophys. Res.*, **91**, 4345–4351, 1986.

Kivelson, M. G. and D. J. Southwood, Hydromagnetic waves and the ionosphere, *Geophys. Res. Lett.*, **15**, 1271–1274, 1988.

Lanzerotti, L. J. and L. V. Medford, Local night, impulsive (Pi 2-type) hydromagnetic wave polarization at low latitudes, *Planet. Space Sci.*, **32**, 135–142, 1984.

Lee, D. H., Dynamics of MHD waves propagation in the low-latitude magnetosphere, *J. Geophys. Res.*, **101**, 15371–15386, 1996.

Lee, D. H., On the generation mechanism of Pi 2 pulsations in the magnetosphere, *Geophys. Res. Lett.*, **25**, 583–586, 1998.

Lee, D. H. and K. Kim, Compressional MHD waves in the magnetosphere: A new approach, *J. Geophys. Res.*, **104**, 12379–12385, 1999.

Lester, M., H. J. Singer, D. P. Smits, and W. J. Hughes, Pi 2 pulsations and the substorm current wedge: Low-latitude polarization, *J. Geophys. Res.*, **94**, 17133–17141, 1989.

Lin, C. A., L. C. Lee, and Y. J. Sun, Observations of Pi 2 pulsations at a very low latitude ($L = 1.06$) station and magnetospheric cavity resonances, *J. Geophys. Res.*, **96**, 21105–21114, 1991.

McPherron, R. L., C. T. Russel, and M. P. Aubry, Satellite studies of magnetospheric substorms on August 15, 1968, Phenomenological model for substorm, *J. Geophys. Res.*, **78**, 3131–3149, 1973.

Osaki, H., K. Takahashi, H. Fukunishi, T. Nagatsuma, H. Oya, A. Matsuoka, and D. K. Milling, Pi 2 pulsations observed from the Akebono satellite in the plasmasphere, *J. Geophys. Res.*, **103**, 17605–17615, 1998.

Saito, T., K. Yumoto, and Y. Koyama, Magnetic pulsation Pi 2 as a sensitive indicator of magnetospheric substorm, *Planet. Space Sci.*, **24**, 1025–1029, 1976.

Samson, J. C. and G. Rostoker, Latitude-dependent characteristics of high latitude Pc 4 and Pc 5 micropulsations, *J. Geophys. Res.*, **77**, 6133–6144, 1972.

Southwood, D. J., Some features of field line resonance in the magnetosphere, *Planet. Space Sci.*, **22**, 483–491, 1974.

Southwood, D. J. and W. F. Stuart, Pulsations at the substorm onset, in *Dynamics of the Magnetosphere*, edited by S.-I. Akasofu, pp. 341–355, D. Reidel, Norwell, Mass., 1980.

Stuart, W. F., A mechanism of selective enhancement of Pi 2's by the plasmapause, *J. Atmos. Terr. Phys.*, **36**, 851–859, 1974.

Stuart, W. F., *Array of Magnetometers in NW Europe, The IMS Source Book*, edited by C. T. Russel and D. J. Southwood, pp. 141–152, 1982.

Sutcliffe, P. R., The association of harmonics in Pi 2 power spectra with the plasmapause, *Planet. Space Sci.*, **23**, 1581–1587, 1975.

Sutcliffe, P. R. and K. Yumoto, On the cavity mode nature of low-latitude Pi 2 pulsations, *J. Geophys. Res.*, **96**, 1543–1551, 1991.

Takahashi, K., S. I. Ohtani, and B. J. Anderson, Statistical analysis of Pi 2 pulsations observed by the AMPTE CCE spacecraft in the inner magnetosphere, *J. Geophys. Res.*, **100**, 21929–21941, 1995.

Yeoman, T. K. and D. Orr, Phase and spectral power of mid-latitude Pi 2 pulsations: evidence for a plasmasphere cavity resonances, *Planet. Space Sci.*, **37**, 1367–1383, 1989.

Yeoman, T. K., M. P. Freeman, G. D. Reeves, M. Lester, and D. Orr, A comparison of mid-latitude Pi 2 pulsations and geostationary orbit particle injections as substorm indicators, *J. Geophys. Res.*, **99**, 4085–4093, 1994.

Yumoto, K., Generation and propagation mechanisms of low-latitude magnetic pulsations—A review, *J. Geosphys.*, **60**, 79–105, 1986.

Yumoto, K., External and internal sources of low-frequency MHD waves in the magnetosphere—A review, *J. Geomag. Geoelectr.*, **40**, 293–311, 1988.

Yumoto, K., Evidence of magnetic cavity Pi 2 waves, *J. Geomag. Geoelectr.*, **42**, 1281–1290, 1990.

Yumoto, K. and the 210° MM Magnetic Observation Group, The STEP 210° magnetic network project, *J. Geomag. Geoelectr.*, **48**, 1297–1309, 1996.

Yumoto, K., K. Takahashi, T. Saito, F. W. Menk, B. J. Fraser, T. A. Potemra, and L. J. Zanetti, Some aspects of the relation between Pi 1–2 magnetic pulsations observed at $L = 1.3 - 2.1$ on the ground and substorm-associated magnetic field variations in the near-earth magnetotail observed by AMPTE/CCE, *J. Geophys. Res.*, **94**, 3611–3618, 1989.

Yumoto, K., S. Watanabe, and H. Oya, MHD responses of a model magnetosphere to magnetopause perturbations, Proc. Res. Inst. Atmos., Nagoya Univ., 37, 17–36, 1990.

Yumoto, K., H. Osaki, K. Fukao, K. Shiokawa, Y. Tanaka, S. I. Soloeyev, G. Krymskij, E. F. Vershinin, V. F. Osinin, and 210° MM Magnetic Observation Group, Correlation of high- and low-latitude Pi 2 magnetic pulsations observed at 210° magnetic meridian chain stations, *J. Geomag. Geoelectr.*, **46**, 925–935, 1994.

Zhu, X. M. and M. G. Kivelson, Analytic formulation and quantitative solutions of the coupled ULF wave problem, *J. Geophys. Res.*, **93**, 8602–8612, 1988.

Zhu, X. M. and M. G. Kivelson, Global mode ULF pulsations in a magnetosphere with a nonmonotonic Alfven velocity profile, *J. Geophys. Res.*, **94**, 1479–1485, 1989.

C.-C. Cheng (e-mail: ccheng@sunws.nhit.edu.tw), J.-K. Chao, and K. Yumoto